

Cite this: DOI: 10.1039/c1sc00531f

www.rsc.org/chemicalscience

PERSPECTIVE

Kinetics and thermodynamics in surface-confined molecular self-assembly

Rico Gutzler,* Luis Cardenas and Federico Rosei*

Received 3rd August 2011, Accepted 21st September 2011

DOI: 10.1039/c1sc00531f

Two-dimensional molecular self-assembly at the liquid/solid interface is a widely employed approach in surface science to pattern surfaces at the nanometre scale. A multitude of supramolecular structures can be realized depending on parameters such as the functionalization of the molecular building blocks, the temperature at which self-assembly takes place, the type of solvent and solute concentration. How these and other parameters influence the kinetics and thermodynamics of the self-assembly process is the subject of this review.

Introduction

Molecular self-assembly is a widely used strategy to pattern and functionalize surfaces at the nanometre scale with applications such as functional nanomaterials and organic electronics.^{1–3} The physisorption of organic molecules onto surfaces and their arrangement into ordered monolayers has been extensively investigated, leading to a myriad of different supramolecular structures with different molecular building blocks, both at the liquid/solid interface and the vacuum/solid interface.^{4–15} Despite numerous investigations following the pioneering work of Foster & Frommer¹⁶ and Rabe & Buchholz,^{17,18} it is not yet possible to deliberately engineer molecular monolayers or to predict the structure of such a monolayer for a given molecular building unit. To tackle these shortcomings, it is important to understand the mechanisms that underlie surface-confined molecular self-assembly. Polymorphism – the formation of two or more distinct crystalline monolayer structures – is one facet of two-dimensional molecular self-assembly that lacks a detailed understanding, although many parameters have been identified that can be used to control polymorphism and to switch between several different polymorphs. A nonexclusive list of these parameters includes the type of solvent,^{19–24} concentration of the molecular building block,^{25–27} molecular interactions,^{28–34} size and structure of the adsorbing molecule,^{30,35–37} type of surface^{38–42} and temperature.^{43–48} Care must be taken to discriminate between polymorphism in three-dimensional and two-dimensional crystals, the latter type being relevant in self-assembled organic monolayers. For example, concentration-dependent polymorphism in 3D cannot occur due to thermodynamic reasons, while it is now a commonly accepted feature in 2D crystallization, as pointed out by Matzger and coworkers.⁴⁹

At the liquid/solid interface, interactions between molecular building blocks, solvent molecules and the surface are crucial in

defining the structure of a monolayer. These interactions constitute one aspect of a complex thermodynamic description of the self-assembly process, which necessarily also includes parameters such as temperature, entropy, or chemical potentials.¹³ Attempts have been made to find suitable thermodynamic models that semi-quantitatively describe isolated experimental results,^{37,47,48,50,51} but, until now, a conclusive and more global thermodynamic description is still lacking. Furthermore, as in any reaction, kinetic factors influence supramolecular self-assembly. Several studies show that kinetically stabilized phases can form at a surface, which over time transform into thermodynamically more stable polymorphs.^{49,52,53} Some of the parameters that govern kinetics and thermodynamics of molecular self-assembly are elucidated here in view of their importance for the self-assembly process.

The complexity of a thorough description of supramolecular self-assembly at surfaces stems from the intricate adsorption process itself. Once the solution is applied to a clean surface, commonly highly oriented pyrolytic graphite (HOPG), the dissolved molecular building units (analyte) start to adsorb on the substrate. They are free to move on the surface and eventually bind to other adsorbed molecules or desorb back into solution. Stable monolayers can be formed when a sufficiently large number of molecules on the surface assemble into large crystalline domains. However, a molecule adsorbed in a monolayer is not necessarily fixed in its position and may desorb back into the bulk solution. The monolayer is thus in a dynamic equilibrium with the solution and constant adsorption/desorption is likely to happen on timescales relevant for experiments.

Parameters such as adsorption/desorption rates, analyte mobility in solution and on the surface and the nucleation rates of different polymorphs can influence the kinetics of the two-dimensional crystallization. Solvation enthalpy, adsorption enthalpy and entropy changes between the dissolved state and adsorbed state of the analyte describe the energetic contribution of surface-confined molecular self-assembly and hence merge into a thermodynamic description. A microscopic picture of the adsorption/surface diffusion processes can be offered for the

Institut National de la Recherche Scientifique, Université du Québec, 1650 boulevard Lionel-Boulet, Varennes, QC, J3X 1S2, Canada. E-mail: gutzler@emt.inrs.ca; rosei@emt.inrs.ca

growth of surface nanostructures from adsorbed species.¹ If the deposition rate, *i.e.* the rate at which molecules adsorb on the surface, is given by F and the surface diffusivity of the adsorbed molecule is given by D , the ratio D/F represents a measure of the average distance a molecule has to travel on the surface before it encounters other molecules, thus forming a nucleus for monolayer growth. A large value of D/F implies quick diffusion and slow adsorption. Equilibrium structures are the consequence, as each molecule has enough time to settle in an energetic minimum. Small values of D/F , on the other hand, result from fast adsorption and little time for diffusion. This regime would stabilize kinetically favoured structures if a metastable energetic minimum is attainable faster than the thermodynamic global minimum. How quick molecules adsorb and how fast they move on the surface defines whether the formed structure is only metastable or if it already is in its thermodynamically most preferred state.

Molecular monolayers can be observed and characterized by scanning probe techniques. The scanning tunnelling microscope (STM) has proven to be a particularly versatile tool for imaging physisorbed molecules.^{54–56} It allows imaging of thin molecular layers adsorbed on electrically conductive surfaces with sub-molecular resolution in real space and with a temporal resolution at the second-scale. Unlike diffraction techniques, the STM does not provide space-averaged information, but allows us to image spatially non-periodic structures and defects, such as grain boundaries, and simplifies the discrimination of coexisting polymorphs within a molecular layer. For instance, slow phase transitions from one polymorph into another composed of the same molecular building block can be observed in real time by STM,^{49,52,53} yielding important information on phase transition kinetics. Studying the dynamic behaviour of the domains of co-adsorbed molecular building blocks facilitates conclusions about the relative energetic stability of polymorphs.^{36,57} Likewise, grain boundary dynamics recorded by STM allows a qualitative insight into molecular interactions within a monolayer.^{58–61} The STM is thus an excellent tool to study the evolution of molecular monolayers and to characterize (*meta*)stable polymorphs.

Kinetic and thermodynamic control over 2D molecular self-assembly

Thermodynamics is concerned with energy differences between static states of a system, while kinetics includes rates of change and thus time-dependent phenomena. Transitions from one polymorph into another, under constant conditions or as a response to external stimuli, are such time-dependent processes the rate of which is determined by an activation energy. Competitive co-adsorption of different analytes and resulting dynamic changes in the relative surface coverage of each molecule is another example that is determined by kinetic factors, such as nucleation rates. Both examples will be discussed in the following sections.

Kinetics and the importance of equilibration time

Successive phase transitions from one initial polymorph into a second one, followed by a transition into a final, third polymorph were observed by STM for the molecule hexakis(*n*-dodecyl)-peri-hexabenzocoronene (HBC-C₁₂, Fig. 1a).⁵²

This molecule adsorbs readily on top of an alkane (*n*-C₅₀H₁₀₂) monolayer adsorbed on HOPG into an oblique structure from a *n*-tetradecane solution (α phase, Fig. 1b). One hour after starting the experiment, only this phase is observable. Within the next hour, the oblique phase transforms into another, different polymorph (β phase, Fig. 1c). Once the transition is completed, the final polymorph (γ phase, Fig. 1d) starts to form, which is the only remaining phase after eight hours. Solvent evaporation was suppressed by using a liquid cell so that the concentration of the solute remained constant. This ensures that the transitions are not induced by an artificial increase in concentration due to solvent evaporation. The authors conclude that the phases α and β are metastable, that γ is the thermodynamically most stable polymorph and that the kinetic barrier between two phases is of the order of the thermal energy (see Fig. 1e for a potential energy diagram). The α phase is the least densely packed structure of HBC-C₁₂, while the γ phase is the most densely packed. For this system, there is a trend towards dense-packed polymorphs as the thermodynamically stable structure; a trend that is likewise observed in the self-assembly of other molecules. Maximizing the number of molecules adsorbed on the surface minimizes energy by exchanging solvation enthalpy with adsorption enthalpy and drives self-assembly towards densely packed monolayers.

Time-dependent phase transitions were also observed for octadecylcarbamic acid tetradecyl ester, a linear molecule, when assembling from phenyloctane solution onto HOPG.⁵³ Two different polymorphs form at the surface, one of which slowly grows at the expense of the other. The authors interpret this conversion in view of Ostwald's rule of stages. This rule describes the initial formation of a kinetically favoured metastable crystal structure and its subsequent transformation into the thermodynamically most stable crystal structure. The polymorph with higher free energy is kinetically more accessible, but changes over time into the other more stable polymorph. Ostwald's rule of stages seems to be applicable not only to this study, but also gives an adequate description of the phase transformations in the HBC-C₁₂ monolayers in the study discussed above and likewise explains the following temperature induced phase transitions.

Temperature

The same molecule assembling on Au(111) from *n*-tetradecane solution shows a time-dependent transition from an initial polymorph (Fig. 2a) to a second polymorph (Fig. 2b), which is completed after one hour.⁴³ Two further transitions can be induced by progressively heating the sample to 50 °C, where at 30 °C a third phase (Fig. 2c) appears and above 35 °C, a fourth, final phase is discernible (Fig. 2d). Above 50 °C, no new phase transitions are observable. The phase transitions are not reversible, *i.e.*, after cooling the annealed surface down to room temperature, imaging still yields the high-temperature phase. Again, care was taken to minimize solvent evaporation by using an environmental chamber saturated with *n*-tetradecane. The first structure that forms is not stable and rapidly transforms into the second polymorph, implying that it is kinetically favoured but thermodynamically unstable. The third phase is more stable than the second phase, but requires additional thermal energy to

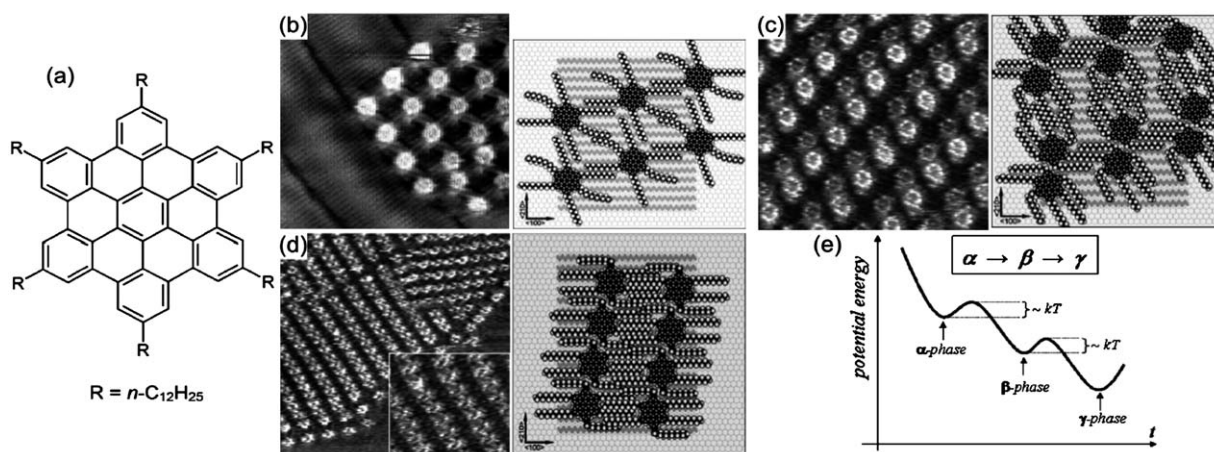


Fig. 1 (a) The chemical structure of hexakis(*n*-dodecyl)-peri-hexabenzocoronene. (b) A STM topograph and molecular model of the self-assembled monolayer of HBC- C_{12} on $n-C_{50}H_{102}$ in the oblique α -phase. The α -phase transforms spontaneously into the β -phase (c), and subsequently into the γ -phase (d). A potential energy diagram of the transitions $\alpha \rightarrow \beta \rightarrow \gamma$ as a function of time is shown in (e). The barrier heights separating the minima of different polymorphs need to be of the order of $k_B T$ to facilitate the phase transitions. See ref. [52]. Reproduced and adapted with permission from the American Chemical Society.

overcome a kinetic barrier. The same holds true for the transition from the third to the final, fourth phase. Phases two and three are metastable with respect to the fourth phase, which is supported by the non-reversibility of the transition. It is apparent from both studies on HBC- C_{12} that kinetic barriers that separate energetically different polymorphs can be surmounted by either waiting for a certain amount of time, or by supplying thermal energy to accelerate the transition process.

Concentration

Structural modifications in molecular monolayers can be induced by changing the environment in which self-assembly takes place. Matzger and coworkers changed *in situ* the concentration of the solution from which the analyte, an amide with an aliphatic chain (Fig. 3a), physisorbs on graphite.⁴⁹ The polymorph that is stable at high concentrations (phase II, Fig. 3b) is destabilized by the addition of pure solvent and re-assembles first into a kinetic phase (phase IV, Fig. 3c), and subsequently into the thermodynamically preferred phase (phase V, Fig. 3d). The addition of pure solvent to the solution effectively reduces the concentration of the analyte in solution, thereby changing the adsorption–desorption equilibrium. The densely packed phase II is destabilized by the addition of solvent and transforms into the polymorph that is stable at the new concentration. Although this polymorph corresponds to phase V, phase IV is formed as an intermediate polymorph, since it is kinetically more easily accessible than phase V. After equilibration times of the order of several minutes, the initially observed coexistence of all three phases disappears and phase V is the only remaining polymorph. Fig. 3e displays a reaction coordinate diagram corresponding to the transition from phase II through the intermediate phase IV and eventually settling into the most stable polymorph phase V. It depicts the relative energetic stability of each polymorph for the concentration at which the transition is observed. Since at no concentration

phase IV is observed as a stable polymorph, it is concluded that it is a kinetic form and not thermodynamically stable.

Competitive coadsorption, nucleation rates and Ostwald ripening

The importance of kinetics can also be observed in competitive adsorption of two different analytes from binary mixture solutions. This differs from the above studies, which describe the adsorption of one type of molecule on the surface and the transition of monolayers made of this building block only. Two or more molecular building blocks, on the other hand, can co-adsorb to form either mixed monolayers where the constituents co-assemble to form one polymorph,^{29,50,62–69} or adsorb to form separate, pure domains of polymorphs consisting of only one type of molecule.^{57,70,71} The latter case, for example, is observable for a binary mixture of the liquid crystal solvent 4'-octyl-4-biphenylcarbonitrile (8CB, Fig. 4a) and *n*-tetracontane ($C_{40}H_{82}$).⁵⁷ Both molecules co-assemble on HOPG, albeit with different nucleation rates. This leads to the ordering of each component into pure domains consisting of one type of molecule. While during the initial stages the largest part of the surface is covered with domains of $C_{40}H_{82}$ and little coverage is due to 8CB, the 8CB domains grow in time at the expense of the $C_{40}H_{82}$ domains (*cf.* Figs 4b–e). After one to two days, the surface is almost completely covered by 8CB. It is also observed that $C_{40}H_{82}$ grows in many small domains, while 8CB assembles into large domains. The conclusion drawn from the time-dependent relative coverage is that the 8CB polymorph is thermodynamically more stable than the $C_{40}H_{82}$ polymorph, since it prevails in the long run. The authors argue that the different sizes of the domains indicate the importance of the nucleation rates and growth rates of each polymorph. Their proposed analytical model defines a ratio $r = R_G/R_N$ between the growth rate, R_G , and nucleation rate, R_N , for both molecular types. A large ratio r for a certain molecular type leads to the formation of well-ordered domains that extend over large areas, as observed for

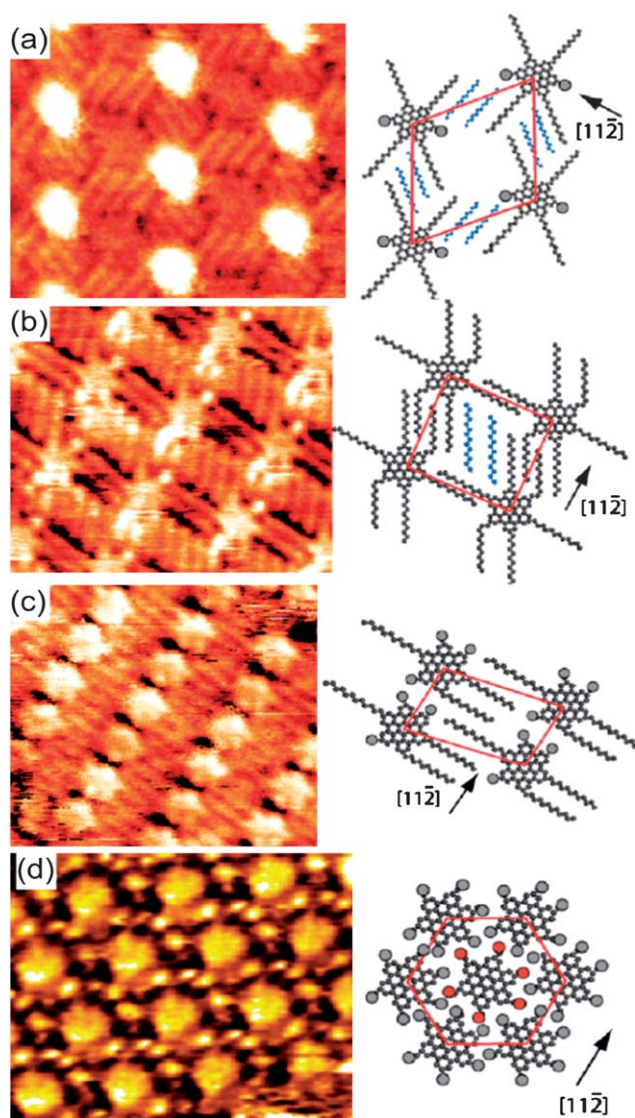


Fig. 2 STM images of the four phases observed for HBC-C₁₂ on Au (111) with models of the molecular structure. (a) The initial first metastable phase, which evolves rapidly into the second phase (b). Heating to 30 °C transforms the second phase into the third phase (c). Above 35 °C, the final and thermodynamically most stable phase appears (d). See ref. [43]. Reproduced and adapted with permission from the American Chemical Society.

8CB. On the contrary, a small ratio r , when domains nucleate quickly but are slow in growth, yields many small domains, which describes the assembly of C₄₀H₈₂. Since in the beginning C₄₀H₈₂ forms many small domains while 8CB almost forms no domains, it can be inferred that $R_N(\text{C}_{40}\text{H}_{82}) > R_N(8\text{CB})$. Nevertheless, in the long run, the molecule with the larger growth rate should eventually cover most of the surface, just as was observed in this study where 8CB eventually displaces the C₄₀H₈₂ domains. A qualitative interpretation of the data in view of nucleation rates and relative thermodynamic stability explains the transition from predominant C₄₀H₈₂ coverage to near complete 8CB coverage. These findings can almost certainly be generalized to the other discussed studies: a fast nucleating

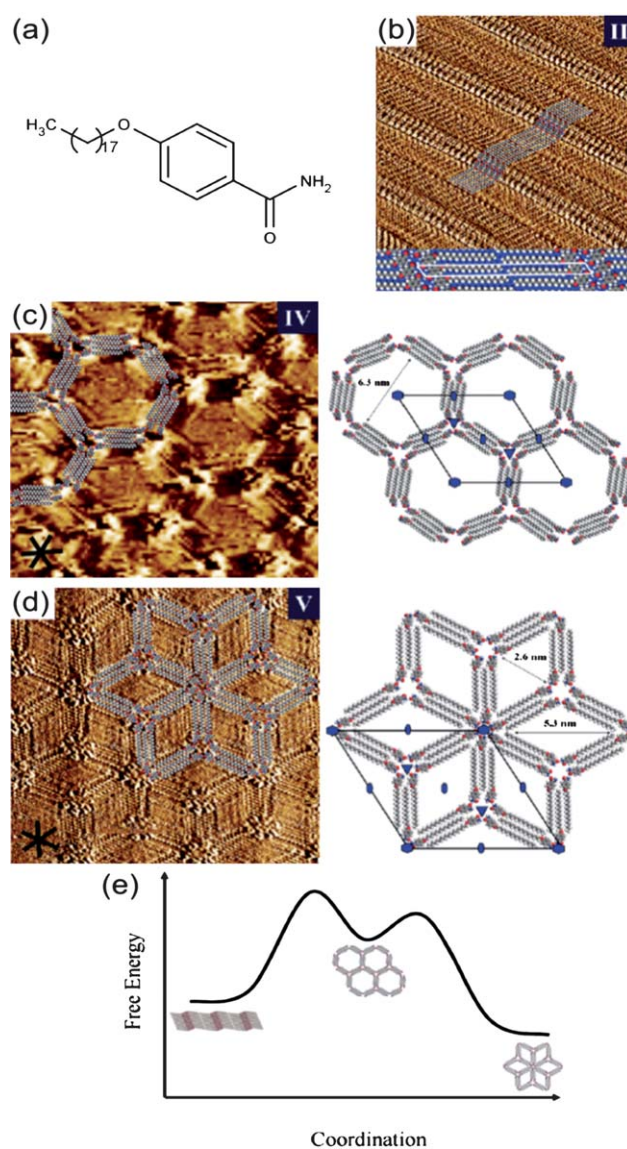


Fig. 3 (a) The chemical structure of the investigated amide. (b) The STM image and computed model of the close-packed phase II assembled from phenyloctane. (c) The porous structure IV that forms upon lowering the concentration of the analyte in solution by adding pure solvent. (d) Subsequent to the formation of phase IV, phase V assembles and remains as the thermodynamic stable polymorph. The transition is schematically shown in a reaction diagram (e), which shows phase IV as a kinetic metastable state in the transition from phase II to the energetically more favorable phase V. See ref. [49]. Reproduced and adapted with permission from the American Chemical Society.

polymorph assembles quickly on the surface, resulting in a high coverage. A different, slower nucleating polymorph, which is otherwise energetically more stable, assembles with a time lag. But since this polymorph is thermodynamically more favourable, it will eventually outgrow the fast nucleating polymorph.

Similar kinetic transitions are observed for multicomponent systems.³⁶ At the heptanoic acid/graphite interface for example, a binary mixture of trimesic acid (TMA, Fig. 5a) and 1-undecanol (Fig. 5b) shows the initial formation of pure TMA domains (Fig. 5c, triangular domain in the centre of each STM image).

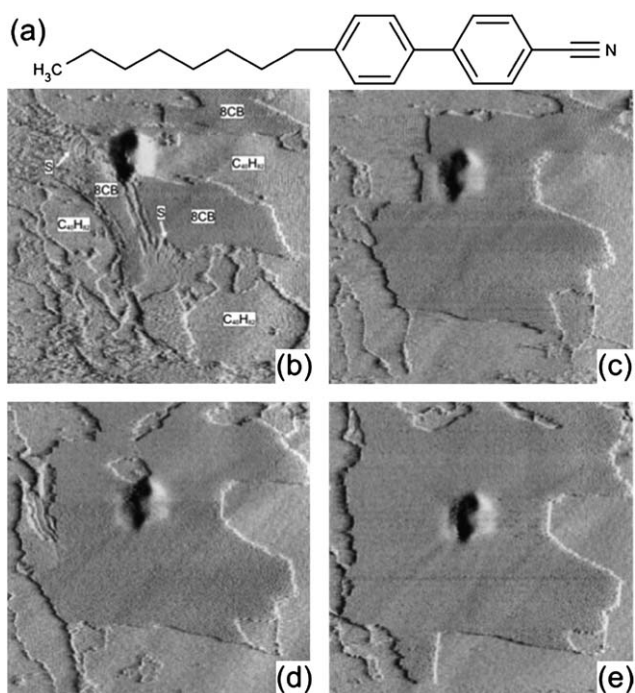


Fig. 4 (a) The chemical structure of 4'-octyl-4-biphenylcarbonitrile. (b) A monolayer of co-adsorbed 8CB and *n*-tetracontane that form separate pure domains. (c–e) Surface coverage of 8CB increases at the expense of *n*-tetracontane and small 8CB domains coalesce into larger domains. Topographs were recorded at 1.7 min time intervals. Reproduced and adapted from ref. [57] with permission from the American Chemical Society.

Over time, these domains gradually dissolve and cede to a monolayer structure comprised of both TMA and 1-undecanol, which surrounds the pure domain. This bicomponent self-assembled network seems to be thermodynamically more stable than the pure TMA domain, arguably due to a higher adsorption enthalpy of the long-chain alcohol compared to TMA. Apart from the open-pore network, also not otherwise observable close-packed structures of TMA could be stabilized within the TMA/alcohol network.⁷² In view of these results, the kinetically preferred pure TMA structure might be favoured in the short term over the mixed structure due to a higher nucleation rate.

Another noteworthy observation on the dynamic behaviour of separated homomolecular domains based on kinetics is Ostwald ripening, which describes the growth of large domains at the expense of small domains.^{59–61,73,74} The driving force is thermodynamic in origin and is due to an evolution towards a minimum in line energy, *i.e.*, minimizing the energy of the boundary of a domain. Molecules at the boundary are commonly less strongly bonded than in the inside of a domain due to a lower number of binding partners. Minimizing the number of molecules at the boundary with respect to the number of molecules inside a domain equals minimizing the overall energy. Since small domains have a larger ratio of molecules at the boundary, with respect to molecules in the inside, than large domains and these outer molecules detach faster than molecules from the inside due to their lower binding energy, small domains shrink while larger domains grow. The kinetic process itself – the detachment of molecules from small domains and their inclusion into larger

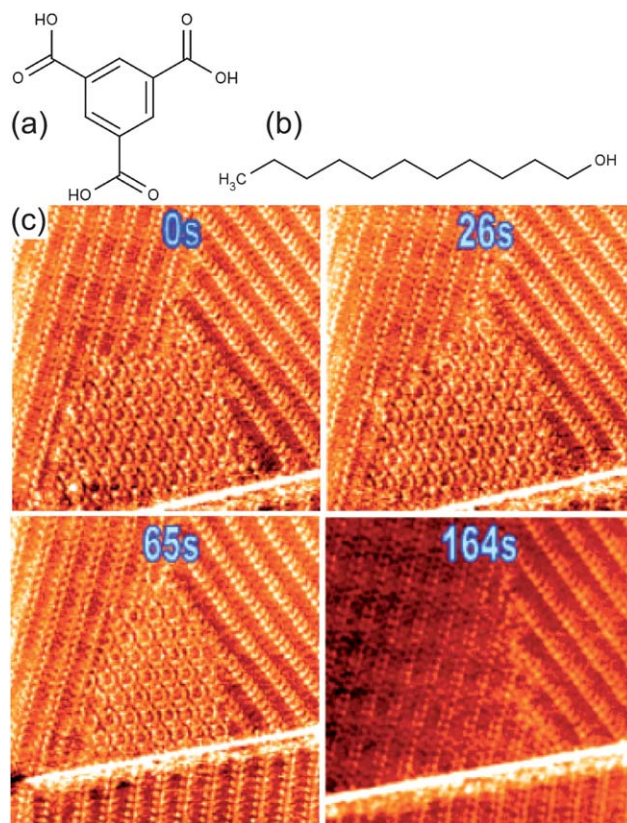


Fig. 5 The chemical structure of (a) TMA and (b) 1-undecanol. (c) STM images showing the growth of the tapes of TMA/1-undecanol SAMNs at the expense of the flower structure consisting of pure TMA. See ref. [36]. Reproduced and adapted with permission from the American Chemical Society.

domains – depends on the rate at which the detachment/attachment occurs. Kinetics allows an understanding of dynamic processes that occur when molecules self-assemble at the liquid/solid interface. But although time-dependent phenomena are encountered in such experiments, they do not constitute the majority of reported observations.

Thermodynamics

Stable self-assembled monolayers are studied quite often and are usually assumed to be thermodynamically controlled. The whole system comprised of surface, solution and self-assembled interfacial monolayer can be characterized in terms of the Gibbs free energy G . A minimum in this state function corresponds to the system being in thermodynamic equilibrium, *i.e.*, the self-assembled molecular layer is in equilibrium with the solution phase. Two descriptions can be encountered in the literature for changes in the Gibbs free energy, one dependent on chemical potentials μ_i

$$\Delta G = \sum_i \mu_i \Delta N_i, \quad (1a)$$

Where N_i is the number of molecules in phase i , and the other in terms of enthalpy H and entropy S

$$\Delta G = \Delta H - T\Delta S, \quad (1b)$$

where T is the temperature. According to Samorì and coworkers, eqn (1a) can be used to express the Gibbs free energy partitioned into three contributions:³⁷ (i) the number of dissolved molecules in solution $N_{i,\text{solvated}}$ with their corresponding chemical potential μ_i , (ii) the area A_i of the surface covered with a molecular layer of type i and its surface free energy γ_i and (iii) the free energy $\gamma_{\text{surface/solvent}}$ of the surface in contact with the solution where no stable molecular layer is formed:

$$G = \sum_i \gamma_i A_i + \sum_i \mu_i N_{i,\text{solvated}} + \gamma_{\text{surface/solvent}} \left(A_{\text{total}} - \sum_i A_i \right) \quad (2)$$

Two different extremes in this model are apparent. The first one corresponds to high-concentration solutions with a much larger number of molecules dissolved compared to adsorbed molecules. In this case, after the formation of a monolayer covering the whole surface, the last term in eqn (2) goes to zero. The Gibbs free energy is then minimized by a balance of the two remaining terms, defined by the chemical potential in solution μ_i and the surface free energy γ_i . Minimizing the surface free energy is achieved through the maximization of the number of molecules on the surface and a maximization of interactions of the molecule per unit area. This scenario is the one encountered most often in the literature. The second case corresponds to low concentrations of the analyte in solution. Under these conditions, the number of molecules in solution above the surface might contain fewer molecules than necessary to cover the entire substrate with a monolayer of a given polymorph. If all molecules adsorb on the surface, the second term in eqn (2) equals zero and the Gibbs free energy depends on a balance between the first and the third term, characterized by the surface free energy of the molecular layer γ_i and the surface free energy of the solvent/surface interface $\gamma_{\text{surface/solvent}}$. The requirement to minimize the surface free energy yields the formation of polymorphs in which each analyte molecule maximizes its interaction in the monolayer. While in the high-concentration regime the interaction energy per unit area is an adequate measure to compare the relative stability of different polymorphs, in the low-concentration regime the molar adsorption energy is more useful. Few experiments have been reported for the latter case of low analyte concentrations.⁶⁵ Samorì's group used eqn (2) to rationalize the formation of bimolecular layers from different building blocks³⁷ and a similar interpretation regarding the adsorption energy per molecule at low analyte concentrations *versus* adsorption energy per unit area at high analyte concentrations was discussed by Matzger and co-workers.^{49,70}

Concentration in a monocomponent system

The thermodynamic equilibrium of the solution/interface system can be changed by tuning parameters, such as concentration, temperature and type of solvent. De Feyter's group investigated the concentration dependence of monolayer formation using alkoxyated dehydrobenzo[12]annulenes (DBAs, Fig. 6a) at the 1,2,4-trichlorobenzene/HOPG interface.²⁵ When assembling from solutions with high DBA concentration, the molecules form a densely packed linear motif (Fig. 6c). At low concentrations, a porous honeycomb network is formed (Fig. 6d) and both

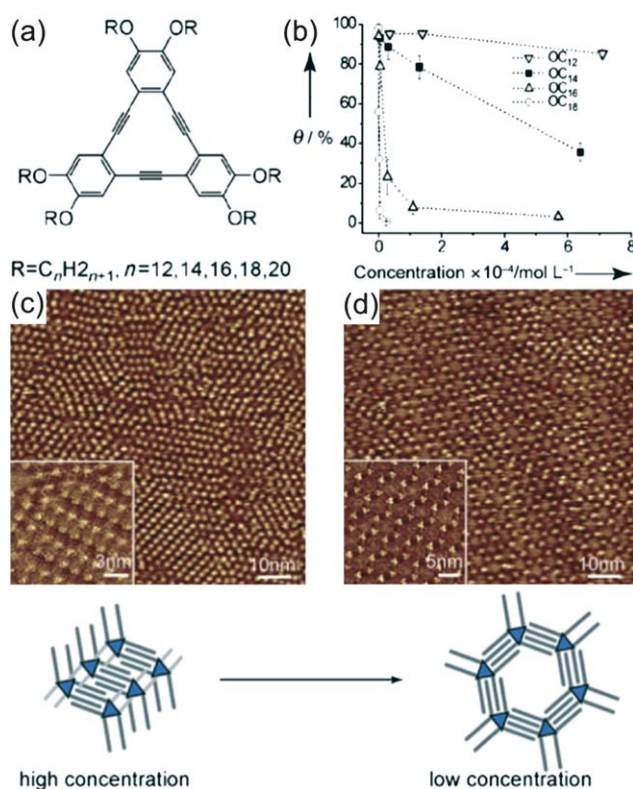


Fig. 6 (a) The chemical structure of alkoxyated dehydrobenzo[12]annulenes. (b) Surface coverage θ dependence of the honeycomb structure on DBA concentration. Low concentrations favor the honeycomb polymorph. (c) STM image and molecular model of the linear structure. (d) STM image and molecular model of the honeycomb structure. See ref. [25]. Reproduced and adapted with permission from Wiley-VCH Verlag GmbH & Co. KGaA.

polymorphs coexist for intermediate concentrations. The relative coverage of the surface of each polymorph can thus be controlled by a deliberate choice of concentration (*cf.* Fig. 6b). A thermodynamic model was derived from a formula similar to eqn (2) that describes how the relative coverage correlates to concentration and temperature. Starting from the assumption of an equilibrium between the two polymorphs and the molecules in solution and assuming full coverage of the surface with molecules, a measure of the relative coverage can be expressed as

$$\frac{Y_h}{Y_l \left(\frac{l}{h}\right)} = e^{\left(\frac{\left(\mu_{0,\text{solution}} - \mu_{0,h} \right) - \left(\frac{l}{h}\right) \left(\mu_{0,\text{solution}} - \mu_{0,l} \right)}{k_B T} \right)} c^{\left(1 - \frac{l}{h}\right)} \quad (3)$$

Y_h is the coverage of the surface with the honeycomb structure, Y_l the part of the surface covered with the linear structure, and h and l are the numbers of molecules per unit area in the respective pattern. $\mu_{0,\text{solution}}$, $\mu_{0,h}$ and $\mu_{0,l}$ are the chemical potentials of the molecules in solution, in the honeycomb and in the linear structure, respectively. As observed by experiment, this formula describes how lowering the concentration c results in increase of the ratio of hexagonal *versus* linear structure Y_h/Y_l (for $l > h$).

The two variables concentration c and temperature T can, in principle, be used to tune the relative coverage. Eqn (3) comprises important parameters that influence the thermodynamic equilibrium and thus govern molecular self-assembly, which depends on the analyte and the solvent. The type of solvent enters the equation through the chemical potential $\mu_{0,\text{solution}}$, which is related to the solvation enthalpy, and $\mu_{0,\text{h}}$, $\mu_{0,\text{l}}$ are characteristic for different analytes and their adsorption geometry on the surface, being related to adsorption enthalpy. The two differences ($\mu_{0,\text{solution}} - \mu_{0,\text{h}}$) and ($\mu_{0,\text{solution}} - \mu_{0,\text{l}}$) in the exponential term delineate how relative chemical potentials of each polymorph influence equilibrium conditions. Since the derivation of eqn (3) is general and is independent of the choice of analyte, solvent, or surface, it should hold in principle for all systems in which one component can assemble into two different polymorphs. The observation that the concentration can be used to control which polymorph assembles on a surface is general and has been confirmed by various other studies.^{24–27,47,50,51,75,76} Generally, low concentrations result in the formation of low-density structures.

Charra *et al.* elaborated on this model to account for their observation of a clear-cut phase transition where only one of two polymorphs is observed, but not both at the same time.⁴⁸ Just like DBA in the previous study described, the molecule TSB3,5 (Fig. 7a) assembles from phenyloctane into one dense and one porous structure (Figs 7b and c). By adjusting the deposition and annealing temperatures, the composition of the monolayer could be tuned. After deposition of TSB3,5 at slightly below room temperature and annealing for one hour at 60 °C, large domains of the thermodynamically more stable densely packed structure

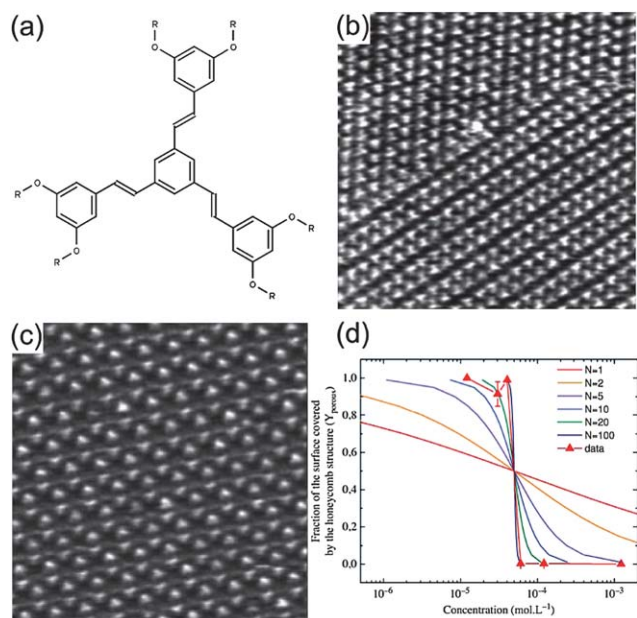


Fig. 7 (a) Chemical structures of TSB (R is an alkyl chain of 6, 8, 10, 12, or 14 carbon atoms). (b) STM topograph of the densely packed structure. (c) STM topograph of the porous structure. (d) The fraction of the surface covered by the porous structure as a function of concentration (red triangles) and model for different values of N (straight lines). See ref. [48]. Reproduced and adapted with permission from the American Institute of Physics.

are observed. In a control experiment, where the solution was applied to the substrate held at 60 °C and allowing equilibration for one hour, large domains of the porous structures are observed. The authors explain this finding as a result of different nucleation and growth rates of the two structures and argue that a kinetic blockade inhibits the transformation from the thermodynamically less stable to the more stable structure, even at elevated temperatures. Based on this finding, the influence of concentration on monolayer formation was studied. The samples were allowed to equilibrate at high temperature (55 °C) to reach thermodynamic equilibrium and subsequently the fraction of the surface covered with each of the two structures was measured. In contrast to the previous study by De Feyter and coworkers, the ratio did not gradually change with concentration but shows a clear phase transition at a critical concentration. Concentrations higher than the critical concentration favoured the formation of only the densely packed structure, while below the critical concentration only the porous structure is observed (Fig. 7d). Eqn (3) was modified accordingly to include this phase transition by taking into account intermolecular interactions within the monolayer. This is done by assuming that not single molecules in solution and in different polymorphs are in thermodynamic equilibrium with each other, but whole domains. This leads to the modified equation

$$\left[\frac{Y_{\text{h}}}{Y_{\text{l}} \left(\frac{l}{h}\right)} \right]^{1/N} = e^{\left(\frac{\left(\mu_{0,\text{solution}} - \frac{1}{N} \mu_{0,\text{h}} \right) - \left(\frac{l}{h}\right) \left(\mu_{0,\text{solution}} - \frac{1}{N} \mu_{0,\text{l}} \right)}{k_{\text{B}} T} \right)} c^{\left(1 - \frac{1}{N}\right)} \quad (4)$$

The newly introduced dimensionless parameter N , which enters the equation through a redefinition of the chemical potential for 2D aggregates of aggregation number N , accounts for molecular interactions that are responsible for the formation of domains rather than disordered structures. Eqn (4) reduces to eqn (3) for the case $N = 1$, *i.e.*, non-interacting particles. This model now reproduces well the observed sharp transition between the two polymorphs for large numbers of N (*cf.* Fig. 7d). The combination of a kinetic interpretation of the nucleation and growth process, as well as the thermodynamic model that explains well the behaviour in equilibrium allow for the assembly of very large and defect free domains of either one of the two polymorphs.

Concentration in a multicomponent system

While the above treatments describe well the assembly of one component into two separate polymorphs, the assembly of two different analytes that co-adsorb into the same polymorph has been investigated by Lackinger and coworkers.⁵⁰ The two carboxylic acid molecules trimesic acid (TMA, Fig. 8a) and 1,3,5-tris(4-carboxyphenyl) benzene (BTB, Fig. 8b) were shown to assemble into six different polymorphs at the solvent/graphite

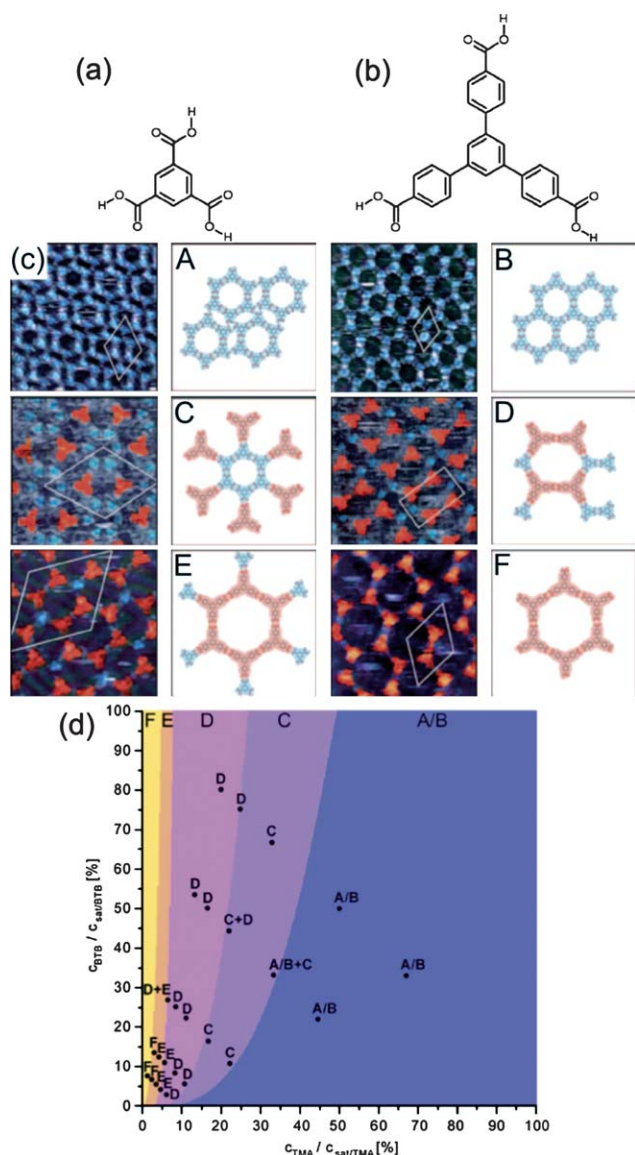


Fig. 8 The chemical structures of (a) TMA and (b) BTB. (c) STM topographs and molecular models of the six different polymorphs A–F that assemble at different concentrations. (d) A phase diagram of the polymorphs A–F. The concentration of TMA is represented by the abscissa, the concentration of BTB by the ordinate. See ref. [50]. Reproduced and adapted with permission from the American Chemical Society.

interface (Fig. 8c). At high TMA/BTB ratios of concentration in solution, two pure TMA polymorphs form, while in the contrary case at low TMA/BTB ratios, one pure BTB polymorph prevails. At intermediate ratios, three further structures form with a composition of TMA and BTB that is governed by the relative amount of TMA and BTB molecule in solution.

Again, a thermodynamic model based on chemical potentials μ_i and number of molecules per unit area in a certain phase σ_i with $i = \text{TMA, BTB}$ was used to rationalize these findings:

$$G = [\sigma_{\text{TMA}}(\text{structure})\mu_{\text{TMA}}(c_{\text{TMA}}) + \sigma_{\text{BTB}}(\text{structure})\mu_{\text{BTB}}(c_{\text{BTB}}) + e_{\text{solvent}}\rho_{\text{cavity}}(\text{structure})]A \quad (5)$$

The area of the covered surface is A , while ρ_{cavity} is the relative cavity area portion and e_{solvent} is an additional free energy per unit area. To derive this formula, the authors approximated the number of molecules in solution as constant and unaffected by the adsorption molecules on the surface. This is justified by the much larger number of molecules in solution compared to the number of molecules at the surface. The second term in eqn (2) thus becomes constant in the calculation of differences in the Gibbs free energy. In eqn (5), apart from the area density σ_i (number of molecules per unit area, see l and h in the above model) in a given structure and the chemical potential μ_i in this structure, an additional third term is introduced to take into account possible solvent co-adsorption in the cavities of the porous structures. This term can thus be related to the third term in eqn (2). Although often no solvent or guest co-adsorption inside cavities of two-dimensional monolayers can be resolved by STM, likely due to short resident times of the molecules in the cavity and their high mobility, co-adsorption is considered to be important in the stabilization of the monolayers. Examples where guest coadsorption in cavities induce changes in the monolayer structure and stabilize otherwise unstable polymorphs underpin the importance of this assumption^{31,77–81} and corroborate the empirical inclusion of the third term. Eqn (5) was used to calculate a phase diagram for TMA/BTB adsorption, which agrees well with experiment (Fig. 8d). The dependence of the monolayer structure on the relative concentration of TMA versus BTB is adequately described by the model and accurately predicts the transition from pure TMA polymorphs to the pure BTB, with three intermediate ones in which both molecules co-assemble when the relative concentration of TMA versus BTB is decreased.

Temperature

The experimental verification of the above discussed models focused primarily on the effect of analyte concentration in solution. However, it is apparent from, for example, eqn (3) that not only concentration but also temperature can be used to control the self-assembly of molecules. This parameter was addressed by Lackinger and co-workers using BTB (Fig. 9a) as the analyte.⁴⁷ BTB assembles from saturated fatty acid solutions into two different polymorphs at room temperature; a dense-packed row structure when heptanoic acid is used as solvent (similar to Fig. 9c), and a hexagonal porous structure when nonanoic acid is used (Fig. 9b). Octanoic acid yields both polymorphs in coexistence. Increasing the temperature at which the molecules adsorb from octanoic acid to about 43 °C resulted in the assembly of the row structure only. This transition is reversible and, after cooling the sample to room temperature, the hexagonal structure reappeared. A similar behavior was found for nonanoic acid, for which the transition from hexagonal to row structure takes place at about 55 °C (see Figs 9b–g for several heat/cool cycles). Both polymorphs, row and hexagonal structure, are assumed to be thermodynamically stable under given conditions and the reversibility of the transition evidences that the low-temperature hexagonal structure is not merely a kinetically trapped polymorph. This stands in contrast to the non-reversible temperature-driven phase transitions observed by Fichou *et al.*⁴³ (*vide supra*), where

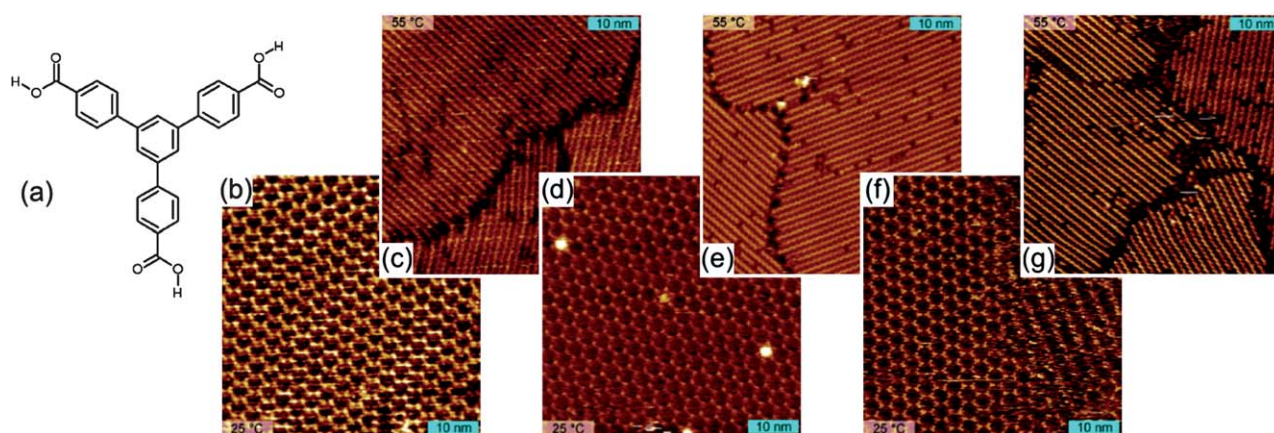


Fig. 9 (a) The chemical structure of BTB. (b–g) Successively recorded STM images of BTB monolayers at the nonanoic acid/graphite interface at various temperatures. (b) The hexagonal porous structure at room temperature. (c) The row structure at about 55 °C. A new cooling to room temperature results in the hexagonal polymorph (d). Repeated heating and cooling cycles are depicted in (e) to (g). See Ref. [47]. Reproduced and adapted with permission from the American Chemical Society.

kinetically stable polymorphs are transformed into thermodynamically stable ones. The thermodynamic model that describes the reversible transition depends on a detailed examination of enthalpic and entropic contributions to the Gibbs free energy in the form of eqn (1b). Molecules that assemble into a static structure on a surface may lower their enthalpy by trading solvation enthalpy for adsorption enthalpy. While this decrease in enthalpy favours the formation of monolayers by minimizing the Gibbs free energy, the loss in entropy upon adsorption acts against it. A molecule in solution possesses translational and rotational degrees of freedom, which are lost, in part, when the molecule sits in a fixed position on a surface. The reduction of degrees of freedom implies a decrease in entropy, which consequently raises the free energy of the system. The loss in entropy at a given temperature has to be compensated for by an adequate reduction in enthalpy for monolayer formation to spontaneously occur. The authors approximate changes in enthalpy through molecular mechanics calculations, a method commonly employed along with *ab initio* calculations to compute the relative energetic stability of different polymorphs.^{27,37,82} Changes in entropy are computed using formulas such as the Sackur–Tetrode equation. This approach allows for the quantitative estimation of differences in the Gibbs free energy for the two phases of BTB and yields the right trend for the phase transition. The transition can only be fully understood using this model if solvent coadsorption is taken into account, which also explains to some extent the solvent-dependent critical temperature at which the transition takes place. Furthermore, analyte concentration in solution was shown to affect the transition and no phase transition at elevated temperatures could be observed in a diluted solution of BTB in nonanoic acid. The model based on detailed estimates of enthalpic and entropic factors to the Gibbs free energy offers an alternative way to the models based on eqn (1a), although both approaches should give the same results. However, quantitative exact considerations have not been reported so far and the modelling of thermodynamics of adsorption in supramolecular chemistry still calls for further research and refinement of models.

Conclusions

Interpretations based on the kinetics and thermodynamics of molecular self-assembly at surfaces have been discussed in several studies and help researchers to understand experimental results. Analytic thermodynamic models are being developed to improve our understanding of supramolecular chemistry in two dimensions. These models might lay the foundation for a more rational approach towards the design of experiments. Time and temperature-dependent irreversible phase transitions have been identified as a transformation of kinetically favourable to thermodynamically stable polymorphs. Nucleation and growth rates have been proposed to be the underlying factors responsible for these observations and naturally lead to a tentative adaptation of Ostwald's rule of stages for two-dimensional supramolecular monolayer growth. Competitive coadsorption of different molecules that assemble into separate domains can be kinetically controlled, as exemplified by the transition from mixed monolayers in which domains of both polymorphs are present to monolayers that almost exclusively contain only one kind of molecule. The fundamental driving force for all of these transitions that are kinetically controlled is the minimization of free energy and can thus be described on thermodynamic grounds. Several models, from purely qualitative to semi-quantitative considerations, are emerging in the literature. They share a detailed description of the analyte in solution and on the surface in terms of chemical potentials, enthalpy and entropy. Several experiments on concentration- and temperature-dependent polymorphism were successfully interpreted on the basis of these models, which could function as a starting point for future refinement. Many parameters that govern molecular self-assembly are still lacking a thorough theoretical and even experimental treatment, such as, for example, the type of solvent and accompanying factors, like solvation enthalpy for thermodynamic considerations, or viscosity and diffusion rates for kinetic considerations. A different, complementary approach towards the understanding of molecular self-assembly is based on Monte Carlo Methods.^{83–86} The information gained from this computational technique allows the prediction of which

polymorph forms under certain conditions. Furthermore, it might help to understand processes such as nucleation and growth, which are too fast to be observed by STM. Two other prominent examples where a thermodynamic and kinetic insight can describe and improve experimental results are random networks/2D glassy systems^{87–89} and the synthesis of ordered surface-confined 2D polymers.^{90–92}

Experimental planning can benefit from a deeper understanding of the underlying mechanisms that control molecular self-assembly and deliberate two-dimensional crystal engineering will be one step closer once kinetics and thermodynamics are fathomed and controlled.

Acknowledgements

Our work is supported by the Natural Sciences and Engineering Research Council of Canada (NSERC) through a Discovery Grant, as well as the Fonds Quebecois sur la Recherche en Nature et Technologies (FQRNT) through a Team Grant and the Ministère du Développement Économique, de l'Innovation et de l'Exportation (MDEIE) through an international collaboration Grant. F. R. is grateful to the Canada Research Chairs program for partial salary support.

Notes and references

- 1 J. V. Barth, G. Costantini and K. Kern, *Nature*, 2005, **437**, 671.
- 2 J. A. A. W. Elemans and S. De Feyter, *Soft Matter*, 2009, **5**, 721.
- 3 A. Ciesielski, C.-A. Palma, M. Bonini and P. Samorì, *Adv. Mater.*, 2010, **22**, 3506.
- 4 M. Surin and P. Samorì, *Small*, 2007, **3**, 190.
- 5 S. Stepanow, N. Lin and J. V. Barth, *J. Phys.: Condens. Matter*, 2008, **20**, 184002.
- 6 T. Kudernac, S. B. Lei, J. A. A. W. Elemans and S. De Feyter, *Chem. Soc. Rev.*, 2009, **38**, 402.
- 7 A. Kühnle, *Curr. Opin. Colloid Interface Sci.*, 2009, **14**, 157.
- 8 M. Lackinger and W. M. Heckl, *Langmuir*, 2009, **25**, 11307.
- 9 Y. L. Yang and C. Wang, *Chem. Soc. Rev.*, 2009, **38**, 2576.
- 10 Y. L. Yang and C. Wang, *Curr. Opin. Colloid Interface Sci.*, 2009, **14**, 135.
- 11 L. Bartels, *Nat. Chem.*, 2010, **2**, 87.
- 12 S. Uemura, R. Tanoue, N. Yilmaz, A. Ohira and M. Kunitake, *Materials*, 2010, **3**, 4252.
- 13 C.-A. Palma, M. Bonini, T. Breiner and P. Samorì, *Adv. Mater.*, 2009, **21**, 1383.
- 14 A. G. Slater, P. H. Beton and N. R. Champness, *Chem. Sci.*, 2011, **2**, 1440.
- 15 L. Cardenas, J. Lipton-Duffin and F. Rosei, *Jpn. J. Appl. Phys.*, 2011, **50**, 08LA02.
- 16 J. S. Foster and J. E. Frommer, *Nature*, 1988, **333**, 542–545.
- 17 J. P. Rabe and S. Buchholz, *Phys. Rev. Lett.*, 1991, **66**, 2096.
- 18 J. P. Rabe and S. Buchholz, *Science*, 1991, **253**, 424.
- 19 F. Jäckel, M. Ai, J. S. Wu, K. Müllen and J. P. Rabe, *J. Am. Chem. Soc.*, 2005, **127**, 14580.
- 20 X. Shao, X. C. Luo, X. Q. Hu and K. Wu, *J. Phys. Chem. B*, 2006, **110**, 1288.
- 21 L. Kampschulte, M. Lackinger, A. K. Maier, R. S. K. Kishore, S. Griessl, M. Schmittl and W. M. Heckl, *J. Phys. Chem. B*, 2006, **110**, 10829.
- 22 W. Mamdough, H. Uji-i, J. S. Ladislav, A. E. Dulcey, V. Percec, F. C. De Schryver and S. De Feyter, *J. Am. Chem. Soc.*, 2006, **128**, 317.
- 23 Y. B. Li, Z. Ma, G. C. Qi, Y. L. Yang, Q. D. Zeng, X. L. Fan, C. Wang and W. Huang, *J. Phys. Chem. C*, 2008, **112**, 8649.
- 24 X. R. Miao, L. Xu, Z. M. Li and W. L. Deng, *J. Phys. Chem. C*, 2011, **115**, 3358.
- 25 S. Lei, K. Tahara, F. C. De Schryver, M. Van der Auweraer, Y. Tobe and S. De Feyter, *Angew. Chem.*, 2008, **120**, 3006.
- 26 K. Tahara, S. Okuhata, J. Adisoejoso, S. B. Lei, T. Fujita, S. De Feyter and Y. Tobe, *J. Am. Chem. Soc.*, 2009, **131**, 17583.
- 27 C. Meier, M. Roos, D. Künzel, A. Breitruck, H. E. Hoster, K. Landfester, A. Gross, R. J. Behm and U. Ziener, *J. Phys. Chem. C*, 2010, **114**, 1268.
- 28 S. B. Lei, C. Wang, S. X. Yin, H. N. Wang, F. Xi, H. W. Liu, B. Xu, L. J. Wan and C. L. Bai, *J. Phys. Chem. B*, 2001, **105**, 10838.
- 29 L. Kampschulte, S. Griessl, W. M. Heckl and M. Lackinger, *J. Phys. Chem. B*, 2005, **109**, 14074.
- 30 K. Tahara, S. Furukawa, H. Uji-i, T. Uchino, T. Ichikawa, J. Zhang, W. Mamdough, M. Sonoda, F. C. De Schryver, S. De Feyter and Y. Tobe, *J. Am. Chem. Soc.*, 2006, **128**, 16613.
- 31 S. Lei, M. Surin, K. Tahara, J. Adisoejoso, R. Lazzaroni, Y. Tobe and S. De Feyter, *Nano Lett.*, 2008, **8**, 2541.
- 32 S.-L. Lee, N.-T. Lin, W.-C. Liao, C.-h. Chen, H.-C. Yang and T.-Y. Luh, *Chem.–Eur. J.*, 2009, **15**, 11594.
- 33 R. Gutzler, S. Lappe, K. Mahata, M. Schmittl, W. M. Heckl and M. Lackinger, *Chem. Commun.*, 2009, 680.
- 34 X. Zhang, T. Chen, H. J. Yan, D. Wang, Q. H. Fan, L. J. Wan, K. Ghosh, H. B. Yang and P. J. Stang, *ACS Nano*, 2010, **4**, 5685.
- 35 M. Lackinger, S. Griessl, T. Markert, F. Jamitzky and W. M. Heckl, *J. Phys. Chem. B*, 2004, **108**, 13652.
- 36 K. G. Nath, O. Ivashenko, J. M. MacLeod, J. A. Miwa, J. D. Wuest, A. Nanci, D. F. Perepichka and F. Rosei, *J. Phys. Chem. C*, 2007, **111**, 16996.
- 37 C.-A. Palma, J. Björk, M. Bonini, M. S. Dyer, A. Llanes-Pallas, D. Bonifazi, M. Persson and P. Samorì, *J. Am. Chem. Soc.*, 2009, **131**, 13062.
- 38 S. Cincotti and J. P. Rabe, *Appl. Phys. Lett.*, 1993, **62**, 3531.
- 39 S. Cincotti and J. P. Rabe, *Supramol. Sci.*, 1994, **1**, 7.
- 40 L. C. Giancarlo, H. B. Fang, S. M. Rubin, A. A. Bront and G. W. Flynn, *J. Phys. Chem. B*, 1998, **102**, 10255.
- 41 Z. X. Xie, X. Xu, B. W. Mao and K. Tanaka, *Langmuir*, 2002, **18**, 3113.
- 42 Z. Q. Zou and F. Chen, *J. Appl. Phys.*, 2008, **103**, 094304.
- 43 C. Marie, F. Sully, L. Tortech, K. Müllen and D. Fichou, *ACS Nano*, 2010, **4**, 1288.
- 44 L. Askadskaya and J. P. Rabe, *Phys. Rev. Lett.*, 1992, **69**, 1395.
- 45 X. H. Kong, K. Deng, Y. L. Yang, Q. D. Zeng and C. Wang, *J. Phys. Chem. C*, 2007, **111**, 9235.
- 46 W. A. English and K. W. Hipps, *J. Phys. Chem. C*, 2008, **112**, 2026.
- 47 R. Gutzler, T. Sirtl, J. F. Dienstmaier, K. Mahata, W. M. Heckl, M. Schmittl and M. Lackinger, *J. Am. Chem. Soc.*, 2010, **132**, 5084.
- 48 A. Bellec, C. Arrigoni, G. Schull, L. Douillard, C. Fiorini-Debuisschert, F. Mathevet, D. Kreher, A. J. Attias and F. Charra, *J. Chem. Phys.*, 2011, **134**, 124702.
- 49 S. Ahn and A. J. Matzger, *J. Am. Chem. Soc.*, 2010, **132**, 11364.
- 50 L. Kampschulte, T. L. Werblowsky, R. S. K. Kishore, M. Schmittl, W. M. Heckl and M. Lackinger, *J. Am. Chem. Soc.*, 2008, **130**, 8502.
- 51 S. B. Lei, K. Tahara, F. C. De Schryver, M. Van der Auweraer, Y. Tobe and S. De Feyter, *Angew. Chem., Int. Ed.*, 2008, **47**, 2964.
- 52 L. Piot, A. Marchenko, J. S. Wu, K. Müllen and D. Fichou, *J. Am. Chem. Soc.*, 2005, **127**, 16245.
- 53 K. Kim, K. E. Plass and A. J. Matzger, *Langmuir*, 2003, **19**, 7149.
- 54 S. De Feyter and F. C. De Schryver, *J. Phys. Chem. B*, 2005, **109**, 4290.
- 55 F. Rosei, M. Schunack, Y. Naitoh, P. Jiang, A. Gourdon, E. Laegsgaard, I. Stensgaard, C. Joachim and F. Besenbacher, *Prog. Surf. Sci.*, 2003, **71**, 95.
- 56 J. V. Barth, *Annu. Rev. Phys. Chem.*, 2007, **58**, 375.
- 57 R. T. Baker, J. D. Mougous, A. Brackley and D. L. Patrick, *Langmuir*, 1999, **15**, 4884.
- 58 A. Stabel, R. Heinz, J. P. Rabe, G. Wegner, F. C. De Schryver, D. Corens, W. Dehaen and C. Sueling, *J. Phys. Chem.*, 1995, **99**, 8690.
- 59 P. Samorì, K. Müllen and H. P. Rabe, *Adv. Mater.*, 2004, **16**, 1761.
- 60 M. Lackinger, S. Griessl, L. Kampschulte, F. Jamitzky and W. M. Heckl, *Small*, 2005, **1**, 532.
- 61 G. M. Florio, J. E. Klare, M. O. Pasamba, T. L. Werblowsky, M. Hyers, B. J. Berne, M. S. Hybertsen, C. Nuckolls and G. W. Flynn, *Langmuir*, 2006, **22**, 10003.
- 62 K. G. Nath, O. Ivashenko, J. A. Miwa, H. Dang, J. D. Wuest, A. Nanci, D. F. Perepichka and F. Rosei, *J. Am. Chem. Soc.*, 2006, **128**, 4212.
- 63 S. L. Xu, M. D. Dong, E. Rauls, R. Otero, T. R. Linderoth and F. Besenbacher, *Nano Lett.*, 2006, **6**, 1434.

- 64 W. Mamdouh, R. E. A. Kelly, M. D. Dong, L. N. Kantorovich and F. Besenbacher, *J. Am. Chem. Soc.*, 2008, **130**, 695.
- 65 C.-A. Palma, M. Bonini, A. Llanes-Pallas, T. Breiner, M. Prato, D. Bonifazi and P. Samorì, *Chem. Commun.*, 2008, 5289.
- 66 M. Li, Y. L. Yang, K. Q. Zhao, Q. D. Zeng and C. Wang, *J. Phys. Chem. C*, 2008, **112**, 10141.
- 67 Y. B. Li, Z. Ma, K. Deng, S. B. Lei, Q. D. Zeng, X. L. Fan, S. De Feyter, W. Huang and C. Wang, *Chem.–Eur. J.*, 2009, **15**, 5418.
- 68 H. Walch, A. K. Maier, W. M. Heckl and M. Lackinger, *J. Phys. Chem. C*, 2009, **113**, 1014.
- 69 S. Xu, S. Yin and S. Xu, *Appl. Phys. A: Mater. Sci. Process.*, 2010, **99**, 99.
- 70 K. Kim, K. E. Plass and A. J. Matzger, *J. Am. Chem. Soc.*, 2005, **127**, 4879.
- 71 S. B. Lei, K. Tahara, Y. Tobe and S. De Feyter, *Chem. Commun.*, 2010, **46**, 9125.
- 72 J. M. MacLeod, O. Ivasenko, D. F. Perepichka and F. Rosei, *Nanotechnology*, 2007, **18**, 424031.
- 73 M. Bonini, L. Zalewski, T. Breiner, F. Dötz, M. Kastler, V. Schädler, M. Surin, R. Lazzaroni and P. Samorì, *Small*, 2009, **5**, 1521.
- 74 R. Heinz, A. Stabel, F. C. De Schryver and J. P. Rabe, *J. Phys. Chem.*, 1995, **99**, 505.
- 75 J. Adisoejoso, K. Tahara, S. Okuhata, S. Lei, Y. Tobe and S. De Feyter, *Angew. Chem., Int. Ed.*, 2009, **48**, 7353.
- 76 S. B. Lei, K. Tahara, J. Adisoejoso, T. Balandina, Y. Tobe and S. De Feyter, *CrystEngComm*, 2010, **12**, 3369–3381.
- 77 S. Furukawa, K. Tahara, F. C. De Schryver, M. Van der Auweraer, Y. Tobe and S. De Feyter, *Angew. Chem., Int. Ed.*, 2007, **46**, 2831.
- 78 D. Bleger, D. Kreher, F. Mathevet, A. J. Attias, G. Schull, A. Huard, L. Douillard, C. Fiorini-Debuischert and F. Charra, *Angew. Chem., Int. Ed.*, 2007, **46**, 7404.
- 79 M. Blunt, X. Lin, M. C. Giménez-López, M. Schröder, N. R. Champness and P. H. Beton, *Chem. Commun.*, 2008, 2304.
- 80 X. R. Miao, L. Xu, Y. J. Li, Z. M. Li, J. Zhou and W. L. Deng, *Chem. Commun.*, 2010, **46**, 8830.
- 81 M. O. Blunt, J. C. Russell, M. C. Giménez-López, N. Taleb, X. Lin, M. Schröder, N. R. Champness and P. H. Beton, *Nat. Chem.*, 2011, **3**, 74.
- 82 J. M. MacLeod, O. Ivasenko, C. Y. Fu, T. Taerum, F. Rosei and D. F. Perepichka, *J. Am. Chem. Soc.*, 2009, **131**, 16844.
- 83 F. Silly, U. K. Weber, A. Q. Shaw, V. M. Burlakov, M. R. Castell, G. A. D. Briggs and D. G. Pettifor, *Phys. Rev. B: Condens. Matter Mater. Phys.*, 2008, **77**, 201408.
- 84 U. K. Weber, V. M. Burlakov, L. M. A. Perdigão, R. H. J. Fawcett, P. H. Beton, N. R. Champness, J. H. Jefferson, G. A. D. Briggs and D. G. Pettifor, *Phys. Rev. Lett.*, 2008, **100**, 156101.
- 85 C. Rohr, M. Balbás Gamba, K. Gruber, E. C. Constable, E. Frey, T. Franosch and B. A. Hermann, *Nano Lett.*, 2010, **10**, 833.
- 86 S. Lei, K. Tahara, K. Müllen, P. Szabelski, Y. Tobe and S. De Feyter, *ACS Nano*, 2011, **5**, 4145.
- 87 M. O. Blunt, J. C. Russell, M. C. Giménez-López, J. P. Garrahan, X. Lin, M. Schröder, N. R. Champness and P. H. Beton, *Science*, 2008, **322**, 1077.
- 88 R. Otero, M. Lukas, R. E. A. Kelly, W. Xu, E. Laegsgaard, I. Stensgaard, L. N. Kantorovich and F. Besenbacher, *Science*, 2008, **319**, 312.
- 89 M. Marschall, J. Reichert, A. Weber-Bargioni, K. Seufert, W. Auwärter, S. Klyatskaya, G. Zoppellaro, M. Ruben and J. V. Barth, *Nat. Chem.*, 2010, **2**, 131.
- 90 D. F. Perepichka and F. Rosei, *Science*, 2009, **323**, 216–217.
- 91 R. Tanoue, R. Higuchi, N. Enoki, Y. Miyasato, S. Uemura, N. Kimizuka, A. Z. Stieg, J. K. Gimzewski and M. Kunitake, *ACS Nano*, 2011, **5**, 3923.
- 92 M. Bieri, M. T. Nguyen, O. Gröning, J. M. Cai, M. Treier, K. Ait-Mansour, P. Ruffieux, C. A. Pignedoli, D. Passerone, M. Kastler, K. Müllen and R. Fasel, *J. Am. Chem. Soc.*, 2010, **132**, 16669.